

OPTIMIZED GRADED SCREEN ARRAY CONFIGURATION FOR PARTICLE SIZE DISTRIBUTION OF RADON PROGENY IN STANDARD CHAMBER

by

Rui CHEN and Shu-Min ZHOU *

Engineering Research Center for Nuclear Technology Application,
East China University of Technology, Ministry of Education, Nanchang, China

Scientific paper

<http://doi.org/10.2298/NTRP181112021C>

Particle size distribution of radon progeny is one of the most important parameters and it needs to be measured accurately. Graded screen array measurement is the most frequently used method for analyzing the characteristics of radon progeny but it needs optimization due to its complex configuration. In this paper, collection efficiency of a single screen and the number of screen array were applied for optimization and simplification of the graded screen array configuration by a series of experimental measurements, theoretical calculations, and standard comparison research methods. When optimized in this way, an experiment was designed for radon progeny particle size distribution in a customized radon chamber. The experiment results indicated that the activity median diameter in unattached mode was 0.81 nm and 287.32 nm in attached mode, which were similar to the results obtained by other researchers. The results prove that the method can satisfy the requirements of graded screen array measurement.

Key words: radon progeny, graded screen array, optimization, activity median diameter

INTRODUCTION

Radon (^{222}Rn) and its progeny are the main sources of natural radiation doses emitted to human body and more than 50 % of the total natural radiation exposure is caused by inhalation of radon and its progeny into human lungs [1]. Compared with ^{222}Rn , its progeny will do more harm to human health after it penetrates the human respiratory system. However, it is difficult to directly measure radon progeny deposited in human respiratory tract due to the nanoscale size distributions of ^{222}Rn progeny in a standard container (such as a radon chamber). The typical particle size distribution of ^{222}Rn progeny, according to present understanding, can be divided into the unattached mode and the attached mode, and the dose per unit exposure for unattached radon progeny is about 25 times higher than that for attached one [2]. Therefore, for accurate analyses of particle size distribution in this range, the graded screen array (GSA) measurement techniques, originated from screen-type diffusion battery measurement, has been introduced to analyze the characteristics of radon progeny by fan model

penetration theory [3]. Unfortunately, the measurement of GSA is too complex to be used in practice.

In this paper, collection efficiency of a single screen and a number of screen arrays were applied for optimization and simplification of GSA configuration with a series of experimental measurements, theoretical calculations, and standard comparison research methods. In this way, we designed an experiment in radon chamber to analyze the particle size distribution of unattached and attached radon progeny. Hence, an experiment was designed for radon progeny particle size distribution in radon chamber. The experiment results indicated that the activity median diameter (AMD) in unattached mode was 0.81 nm and 287.32 nm in attached mode, which were similar to the results of other researchers. The results proved that the method can satisfy the requirements of GSA measurement.

MATERIAL AND METHODS

Optimization of single screen collection efficiency

Due to different particle size range of radon progeny and aerosol, the main mechanism of action for the

* Corresponding author; e-mail: smzhou@ecut.edu.cn

collection by mesh fiber is also infinitely varied. Traditionally, a size range of 0.1~1000 nm can be logarithmically divided into 64 size intervals according to the research of Fukutsu and Tokonami in order to obtain the result of bi-modal particle size distribution [4]. In this paper, for the sake of simplification, the mesh collection efficiency was calculated according to the particle size of the aerosol into three particle size ranges: 0.1~100, 100~200, and 200~1000 in nanometers. In the range of 0.1~100 nm, the research of Fukutsu [5] and Ramamurthi [6] showed that the main mechanism of a single screen is the diffusion effect for the particle size of aerosol in this range. Accordingly, the collection efficiency, P , within the range of particle size can be defined as

$$P = 1 - \exp\left[-\frac{10.8ah}{\pi(1-\alpha)^{1/3}} \frac{66.67Q}{\pi d^2} \frac{d_f^{5/3}}{3\pi\mu d_p} \frac{kTC}{\kappa^{1/2} Pe^{1/2} d_f^{2/3}}\right] \quad (1)$$

where α is the solid volume fraction of screen, h [cm] – the thickness of screen fabric, Q [$L \text{ min}^{-1}$] – the volumetric flow rate, d – the diameter of screen effective collection area in GSA (taking 3.73 normally), d_f [cm] – the fluid flow cross-section diameter of diffusion battery, k [$=1.38 \cdot 10^{-23} \text{ J mol}^{-1} \text{ K}^{-1}$] – the Boltzmann constant, T [K] – thermodynamic temperature, C – the slip coefficient, μ – the gas viscosity coefficient ($\text{g cm}^{-1} \text{ s}^{-1}$, taking $1.89 \cdot 10^{-4}$ normally), and d_p [cm] – related to the particle diameter.

At the range of 100~200 nm, according to the research of Cheng and Yeh [7], the inertial term is negligible when particle size of aerosol is below 200 nm. Therefore, P can be expressed as

$$P = 1 - \exp\left[-\frac{4\alpha h}{\pi(1-\alpha)d_f} \frac{2.7Pe^{2/3}}{kd_f^2} \frac{d_p^2}{\kappa^{1/2} Pe^{1/2} d_f^{2/3}}\right] \quad (2)$$

where Pe is Peclet number and κ is defined as

$$\kappa = \frac{1}{2} \ln \frac{2\alpha}{\pi} \frac{2\alpha}{\pi} \frac{3}{4} \frac{\alpha}{\pi}^2$$

At the range of 200~1000 nm, there is a need to consider the interaction of four mechanisms such as diffusion, interception, inertial collision, and the interaction of diffusion and interception. Namely, the collection efficiency P can be written as

$$P = 1 - \exp\left[-\frac{4\alpha h}{\pi(1-\alpha)d_f} \frac{f(R)}{2\kappa} I \frac{St}{4\kappa^2} \frac{1.24d_p^{2/3}}{\kappa^{1/2} Pe^{1/2} d_f^{2/3}}\right] \quad (3)$$

where St is Stokes number and $f(R)$ is defined as

$$f(R) = (1-R)^{-1} (1-R)^{-2} (1-R) \ln(1-R) \quad (4)$$

where R is the coefficient of interception parameter which is defined as $R = d_p/d_f$.

In order to illustrate the correctness of the calculation results of the collection efficiency of aerosol particles collected in this stage, the sampling flow rate of 3 $L \text{ min}^{-1}$ was selected, and the results of two calculation methods including 30-, 100-, 250-, and 400-mesh collection efficiency were compared. The results of 400-mesh is shown in fig. 1, along with the collection efficiency of radon particles in the range of 0.1~1000 nm obtained by using Fukutsu's method, and the radon particle size ranges of 0.1~100, 100~200 and 200~1000 nm by using our 3-section method.

As shown in fig. 1, the results of efficiency are virtually the same when these methods are used and the max relative error is below 0.2% when $d_p = 10$ nm. We can also see that the collection efficiency of $d_p = 400$ nm under the sample flow rate of 3 $L \text{ min}^{-1}$ is the lowest, collection efficiency is improved when $d_p > 400$ because inertia effect increases as particle size increases.

In general, based on the previous single screen collection efficiency, 5 types of sample flow rates and 6 types of meshes are compared in tab. 1. It indicates that the semi-cut off diameter (the particle size at collection efficiency $p = 50\%$) is decreasing as sampling flow grows by the diffusion process. In this paper, we chose 3 $L \text{ min}^{-1}$ sampling flow rate and 4-layer meshes including 30, 100, 250, and 400 as the parameters of GSA, due to the sampling flow rate of 1 $L \text{ min}^{-1}$ and 2 $L \text{ min}^{-1}$, and the semi-cut off diameter of the first-stage screen which is too large and not fine enough. The overall half-cut particle size at the sampling flow rate of 5 $L \text{ min}^{-1}$ is too small to contain the 5 nm particle size interval of the unbound scorpion aerosol. The half cut-off diameters determined by 30-, 100-, 250-, and 400-mesh at a sampling flow rate of 3 $L \text{ min}^{-1}$ are 0.95, 2.29, 4.28, and 5.48 nm, respectively, which is most suitable for unbound states compared to other combinations with the closest arithmetic progression.

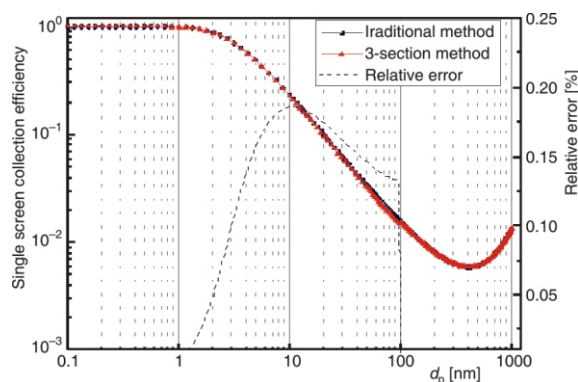


Figure 1. Calculation results of 400-mesh wire collection efficiency with sampling flow rate of 3 $L \text{ min}^{-1}$

Table 1. Semi-cut off diameter [nm] of alternative screens at different sampling flow rates

Sample flow rates [Lmin ⁻¹]	30 meshes	60 meshes	100 meshes	250 meshes	400 meshes	500 meshes
1	1.93	3.19	3.98	7.45	9.55	9.40
2	1.25	2.25	2.81	5.26	6.73	6.63
3	0.95	1.84	2.29	4.28	5.48	5.40
4	0.77	1.51	1.98	3.71	4.74	4.67
5	0.66	1.32	1.72	3.32	4.24	4.18

Cascade screen collection efficiency calculation

According to previous analysis, the collection efficiency of the aerosol of the radon progeny is related to the mesh number and aerosol particle size. Further, radon progeny aerosol particle size can be divided into 64 sections according to Fukutsu's research. Consequently, we collected 64 sections of aerosol particle sizes by a 4-layered mesh and the collection efficiency can be defined as $P_{i,j}$ of section j of particles on the i -th layer screen of GSA.

Based on the previous analysis, the collection efficiency was calculated of the aerosol particles of each particle size segment of the GSA system at sampling flow rate of 3 L min⁻¹. The parameters of $P_{i,j}$ and the total collection efficiency for each particle size segment is shown in fig. 2. The collection efficiency of GSA for the first 20 sections is close to 100 %, and the efficiency from section 27 to 40 (equivalent of 4.532~29.427 nm) noticeably changed. In this paper, we chose the particle size of 9.811 nm at sampling flow rate of 3 Lmin⁻¹.

Backstepping of particle size distribution of aerosol

The GSA sampling and experimental measurements are often used to calculate the activity of the progeny collected from each layer of the screen and the total activity from the sampling. In this paper, we needed to calculate the activity particle size distribution of aerosol particles. Twomey algorithm and ex-

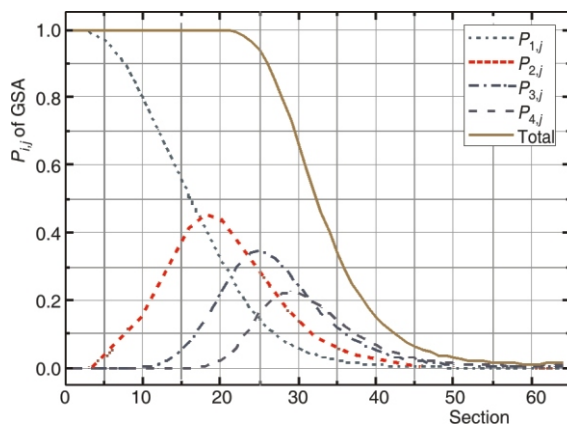


Figure 2. The collection efficiency $P_{i,j}$ of radon progeny particles in GSA configuration

ception maximization (EM) algorithm are more suitable for analyzing the particle size distribution of radon information [8]. Hence in this paper, based on the algorithm of EM, the iterative calculation was carried out by the convergence judgment of effective times. In this way, the activity particle size distribution of the aerosol particles was calculated effectively.

Based on EM algorithm, the activity expectation E of the radon progeny in j th section and on i th layer can be defined as follows

$$E(Z_{i,j}) = Z_0 P_{i,j} f_j \tag{5}$$

where Z_0 is the total activity of sampling of radon progeny aerosol particles, f_j being the proportion of radon progeny aerosol activity in particle size of section j related to total activity. In fact, we often measure the total activity of each layer Z_i instead of $Z_{i,j}$, namely,

$$E(Z_i) = Z_0 \sum_{j=1}^{64} P_{i,j} f_j \tag{6}$$

where $Z_0 = Z_1 + Z_2 + Z_3 + Z_4 + Z_{\text{filter}}$.

For 4-layered single screen, the activity expectation is

$$E(Z_j) = \sum_{i=1}^4 Z_0 P_{i,j} f_j = Z_0 f_j P_j \tag{7}$$

Accordingly, the proportional initial estimation of radon progeny aerosol activity at section j is

$$\hat{f}_j^1 = \frac{z_j}{z_0 P_j} \tag{8}$$

For eq. (6), Z_0 can be rewritten as

$$Z_0 = \sum_{j=1}^{64} \frac{z_i}{P_{i,j} \hat{f}_j^1} \tag{9}$$

the formula applies a variable substitution with eq. (9) to eq. (5) as

$$E(Z_{i,j}) = \frac{z_i}{\sum_{j=1}^{64} P_{i,f} \hat{f}_f^1} P_{i,j} \hat{f}_j^1 \tag{10}$$

And total activity can be expressed as

$$E(Z) = \sum_{i=1}^4 \frac{z_i}{\sum_{j=1}^{64} P_{i,f} \hat{f}_f^1} P_{i,j} \hat{f}_j^1 \tag{11}$$

Based on the iteration ruler, the proportion of radon progeny aerosol activity in particle size of section j related to total activity at the k th time is

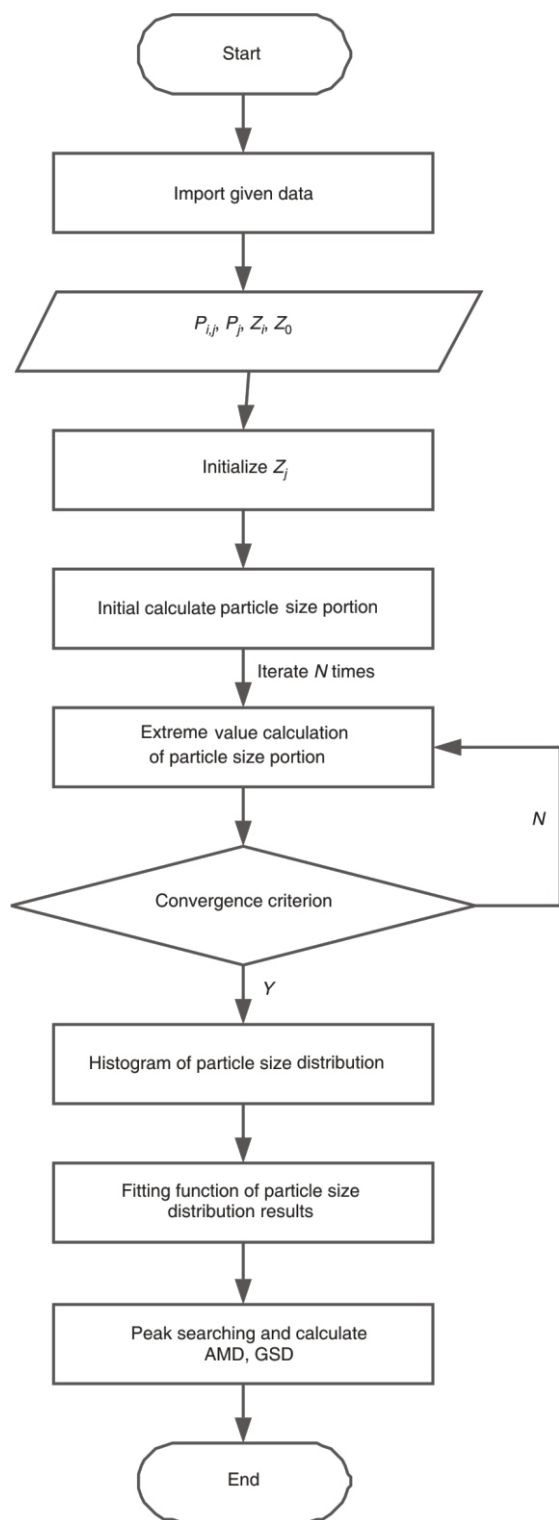


Figure 3. The flowchart of backstepping of particle size distribution of aerosol

$$\hat{f}_j^k = \frac{z_j}{z_0 P_j} \frac{\hat{f}_j^{k-1}}{Z_0 P_{j-1}} \frac{z_i}{P_{i,f} \hat{f}_j^{k-1}} P_{i,j} \quad (12)$$

The overall procedure of this method can be illustrated as in fig. 3

RESULTS AND DISCUSSION

The experiment in this paper was based on the HD-6 multi-functional self-control chamber, developed by East China University of Technology, and the monodisperse 5 % NaCl aerosol particles were added by model 3079 aerosol generator which is manufactured by TSI Inc. The effective volume of the chamber was 4.18 m³ with 10 quick-change joint sampling ports at the front figs. 4 and 5. After the temperature and humidity in the box were stabilized (at 20 % and 30 % RH for this experiment), the initial enthalpy concentration and target enthalpy concentration were input into the box, and the control software automatically calculated the compensation time and performed a certain error. The dynamic compensation in the range made the indoor radon concentration maintain dynamic stability within the control error, and the effective regulation range of the radon concentration was 200~20000 Bqm⁻³ (6000 Bqm⁻³ for this experiment). In this paper, we analyzed the aerosol particle size distribution of radon progeny in this chamber.

The experiment proceeded as follows: (a) the screen with 30-, 100-, 250-, and 400-meshes in increasing order was applied in GSA sampler. Besides, a gas flowmeter was installed between the sampler and air pump to keep the sampling speed of 3 L min⁻¹ for 10 minutes. (b) the number of α particle was recorded on cascade screens at a certain time span. The result are shown in tab. 2.

By applying this data into the backstepping method of particle size distribution of aerosol, we could obtain the value of each fi in different sections. The particle size distribution of the average number is depicted in fig. 6, where dA is the activity concentration of radon progeny multiplied by fi.

There are two peaks in fig. 7, which represented the unattached mode and the attached mode of radon progeny separately. For the peak generated in unattached mode, we calculated that the AMD was 0.81 nm and geometric standard deviation (GSD) was 1.72 by Gaussian curve fitting. In the same way, the

Table 2. The experiment data (alpha particle counters) of radon progeny aerosol particle collected by GSA sampler

Experiment No.	Time span [min]				
	2-5	7-10	12-15	17-20	22-25
1	18	11	5	4	57
2	18	12	5	5	52
3	19	11	4	8	44
Average	18.33	11.33	4.67	5.67	51

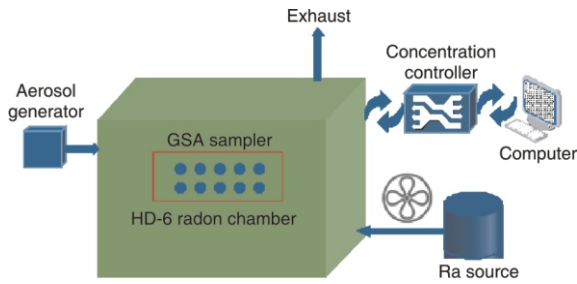


Figure 4. The simulation of the process of HD-6 multi-functional self-control chamber



Figure 5. The environment of experimental measurement

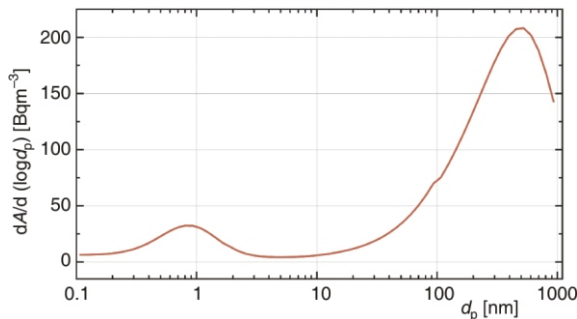
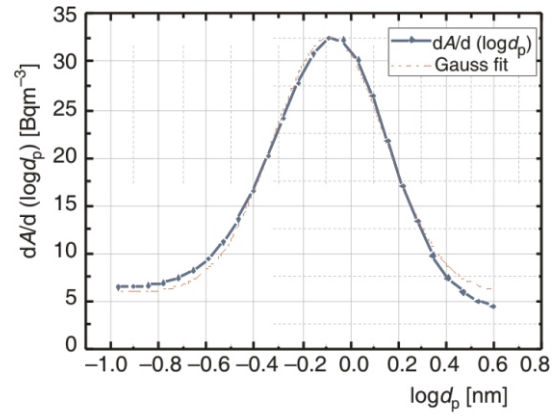


Figure 6. The result of radon progeny aerosol particle size distribution measurement by GSA

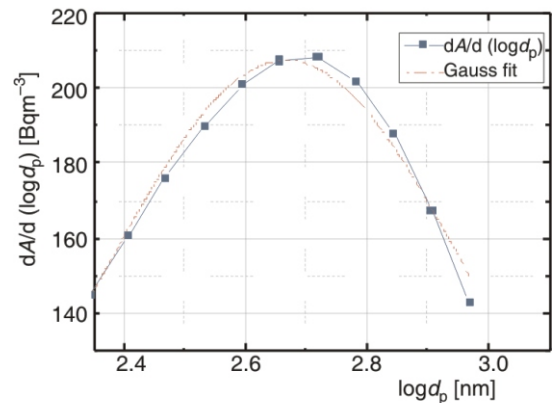
AMD in attached mode was 287.32 nm and GSD was 1.98, which were similar to the results of other researchers [9-11]. The results prove that the method can satisfy the requirements of GSA measurement.

CONCLUSION

In this paper, several optimal methods including optimization of single and cascade screen collection efficiency as well as backstepping of particle size distribution of aerosol for GSA configuration are proposed, which can simplify the calculation process of collection efficiency. Based on HD-6 chamber, the experiment results, 0.81 nm of AMD in unattached mode



(a) Unattached radon progeny aerosol



(b) Attached radon progeny aerosol

Figure 7. The AMD analysis of radon progeny aerosol particles by Gaussian curve fitting

and 287.32 nm of AMD in attached mode, are similar to the results of other researchers, which proves that the method can satisfy the requirements of GSA measurement.

ACKNOWLEDGEMENT

This work was supported by the National Key R&D Program of China (No. 2017YFF0104200), the National Natural Science Foundation of China (No. 11565002), and the Open Funds of Engineering Research Center of Nuclear Technology Application of the Ministry of Education (No. HJSJYB2017-2).

AUTHORS' CONTRIBUTIONS

R. Chen and S. Zhou designed and performed the research and analyzed the data. The paper was written by R. Chen.

REFERENCES

[1] ***, Sources, Effects and Risks of Ionizing Radiation UNSCEAR 2017 report, United Nations Scientific Committee on the Effects of Atomic Radiation, March, 2018

- [2] Yuness, M., *et al.*, Indoor Activity Size Distribution of the Short-Lived Radon Progeny, *Stochastic Environmental Research & Risk Assessment*, 30 (2016), 1, pp. 167-174
- [3] Birchall A., James A. C., Uncertainty Analysis of the Effective Dose Per Unit Exposure from Radon Progeny and Implications for ICRP Risk-Weighting Factors, *Radiation Protection Dosimetry*, 53 (1994), 1-4, pp. 133-140
- [4] Fukutsu, K., *et al.*, Newly Designed Graded Screen Array for Particle Size Measurements of Unattached Radon Decay Products, *Review of Scientific Instruments*, 75 (2004), 3, pp. 783-787
- [5] Fukutsu, K., *et al.*, A New Graded Screen Array for Radon Progeny Size Measurements and Its Numerical Verification, *Journal of Atmospheric Electricity*, 23 (2003), 2, pp. 49-56
- [6] Ramamurthi, M., Simulation Studies of Reconstruction Algorithms for the Determination of Optimum Operating Parameters and Resolution of Graded Screen Array Systems, *Aerosol Science and Technology*, 12 (1990), 3, pp. 700-710
- [7] Cheng, S., Yeh, C., Theory of a Screen Type Diffusion Battery, *Journal of Aerosol Science*, 11 (1980), 3, pp. 313-320
- [8] Maher, E. F., Nan, M. L., EM Algorithm Reconstruction of Particle Size Distributions from Diffusion Battery Data, *Journal of Aerosol Science*, 16 (1985), 6, pp. 557-570
- [9] Tokonami, S., Determination of the Diffusion Coefficient of Unattached Radon Progeny with a Graded Screen Array at the EML Radon/Aerosol Chamber, *Radiation Protection Dosimetry*, 81 (1999), 4, pp. 285-290
- [10] Kranrod, C., Measurement of Radon and Thoron Progeny Size Distributions and Dose Assessments at the Mineral Treatment Industry in Thailand, *Journal of Radioanalytical & Nuclear Chemistry*, 296 (2013), 2, pp. 625-630
- [11] Yuness, M., *et al.*, Indoor Activity Size Distribution of the Short-Lived Radon Progeny, *Stochastic Environmental Research & Risk Assessment*, 30 (2016), 1, pp. 167-174

Received on November 12, 2018
Accepted on May 16, 2019

Жуеј ЧЕН, Шу-Мин ЦОУ

**ОПТИМИЗОВАНА КОНФИГУРАЦИЈА СТЕПЕНАСТЕ МРЕЖЕ
ПРОЗОРА ЗА ДИСТРИБУЦИЈУ ПОТОМАКА РАДОНА ПРЕМА
ВЕЛИЧИНИ ЧЕСТИЦЕ У СТАНДАРДНОЈ КОМОРИ**

Расподела величине честица потомака радона један је од најважнијих параметара и захтева високу прецизност приликом мерења. Мерења применом степенасте мреже прозора најчешће је коришћена метода за анализу карактеристика потомака радона коју је потребно оптимизовати услед комплексне конфигурације. У овом раду испитана је ефикасност прикупљања појединачног прозора као и низа различитог броја прозора ради оптимизације и поједностављења конфигурације степенастог низа прозора на основу серије експерименталних мерења, теоријских прорачуна и стандардних метода поређења резултата. Експеримент је направљен за дистрибуцију потомака радона према величини честице у прилагођеној комори за радон. Резултати експеримента показују да је медијана пречника у неприлагођеном режиму 0.81 nm, а у прилагођеном режиму 287.32 nm, што су вредности сличне добијеним од стране других истраживача. Резултати показују да ова метода може задовољити захтеве мерења степенастим низом прозора.

Кључне речи: потомак радона, степенаста мрежа прозора, оптимизација, медијана пречника